Distinct Electronic Structure of the Electrolyte Gate-Induced Conducting Phase in Vanadium Dioxide Revealed by High-Energy Photoelectron Spectroscopy

Julie Karel,[†,⊥] Carlos E. ViolBarbosa,[†,⊥] Janos Kiss,[†] Jaewoo Jeong,[‡] Nagaphani Aetukuri,[‡] Mahesh G. Samant,[‡] Xeniya Kozina,[§] Eiji Ikenaga,[§] Gerhard H. Fecher,[†] Claudia Felser,[†] and Stuart S. P. Parkin[‡,∞,*]

[†]Max-Planck-Institut für Chemische Physik fester Stoffe, Dresden, Germany 01187, [‡]IBM Almaden Research Center, San Jose, California 95120, United States, [§]Japan Synchrotron Radiation Research Institute, SPring-8, Hyogo, Japan 679-5148, and [∞]Max Planck Institute of Microstructure Physics, Halle, Germany 06120. [⊥]These authors contributed equally to this work.

ABSTRACT The development of new phases of matter at oxide interfaces and surfaces by extrinsic electric fields is of considerable significance both scientifically and technologically. Vanadium dioxide (VO_2), a strongly correlated material, exhibits a temperature-driven metal-to-insulator transition, which is accompanied by a structural transformation from rutile (high-temperature metallic phase) to monoclinic (low-temperature insulator phase). Recently, it was discovered that a low-temperature conducting state emerges in VO_2 thin films upon gating with a liquid electrolyte. Using photoemission spectroscopy measurements of the core and valence band states of electrolyte-gated VO_2 thin films, we show that electronic features in the gate-induced conducting phase are distinct from those of the temperature-induced rutile metallic phase. Moreover, polarization-dependent measurements reveal that the V 3d orbital ordering, which is characteristic of the monoclinic insulating phase, is partially preserved in the gate-induced metallic phase, whereas the thermally induced metallic phase displays no such orbital ordering. Angle-dependent measurements show that the electronic structure of the gate-induced metallic phase persists to a depth of at least ~40 Å, the escape depth of the high-energy photoexcited electrons used here. The distinct electronic structures of the gate-induced and thermally induced metallic phases in VO_2 thin films reflect the distinct mechanisms by which these states originate. The electronic characteristics of the gate-induced metallic state are consistent with the formation of oxygen vacancies from electrolyte gating.

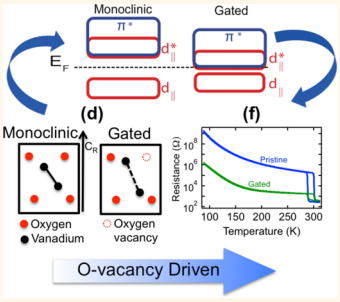

KEYWORDS: VO_2 · ionic liquid electrolyte gating · orbital polarization · X-ray photoelectron spectroscopy

Because of its electronic and structural phase transitions near room temperature, VO_2 has been of intense interest from a fundamental physics viewpoint,[1] where it acts as a model system to investigate the interactions between spin, charge, and orbital degrees of freedom, and as a material for future electronic devices.[2−8] The mechanism driving the metal-to-insulator transition (MIT) is still debated; both electron correlation and lattice distortion effects are expected to play a role.[6,9] The interplay between the crystal structure and electronic properties is depicted in Figure 1. In the tetragonal rutile phase, the V 3d t_{2g} orbitals are crystal-field split into an a_{1g} ($d_{||}$) orbital and doubly degenerate e_g^{π} orbitals.[3−5,10] The $d_{||}$ states are situated parallel to the rutile *c*-axis and originate from the overlapping d orbitals of V atoms within neighboring oxygen octahedra. The e_g^{π} states hybridize with the O 2p orbitals (V−O overlap) to form bonding (π) and antibonding (π^*) states. As shown in Figure 1b for the rutile structure, both the $d_{||}$ and π^* bands cross the Fermi energy (E_F). In the rutile → monoclinic phase transition, V atoms dimerize and the V−V dimers rotate with respect to the rutile *c*-axis (Figure 1a), resulting in the $d_{||}$ bands (formed by V−V overlap) splitting into bonding ($d_{||}$) and antibonding ($d_{||}^*$) states. The displacement of V atoms within their oxygen octahedra also leads to an increased overlap between the V 3d and

* Address correspondence to stuart.parkin@us.ibm.com, stuart.parkin@mpi-halle.mpg.de.

Received for review February 2, 2014 and accepted May 21, 2014.

Published online May 21, 2014
10.1021/nn501724q

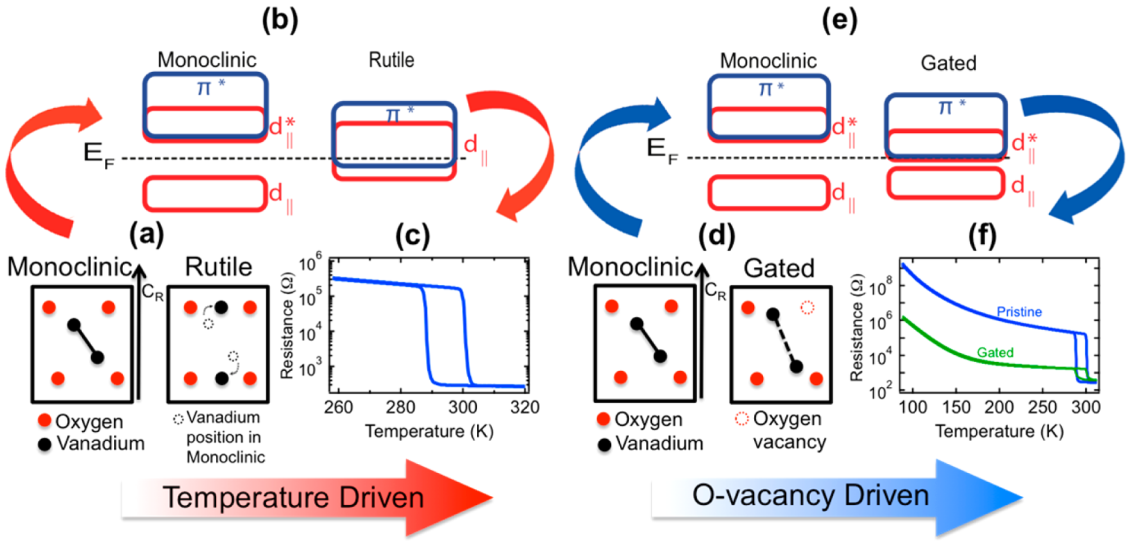

Figure 1. Interconnection between crystal, electronic structure, and transport properties across the insulator−metal transition in VO_2. (a) Schematic illustration of structural changes in the temperature-driven MIT: V atoms, dimerized in the monoclinic structure, become equidistant and form a chain aligned along the *c*-axis (C_R) of the rutile structure. (b) Energy band diagrams reflecting the structural changes (see the text). (c) Temperature dependence of resistivity, showing the strong decrease of resistivity through the temperature-driven MIT. (d) Structural changes induced by electrolyte gating: the electrochemical reaction produces oxygen vacancies in VO_2. In the gated structure, the V−V distances are larger than in the monoclinic phase. (e) Modifications in the band diagram can be described by a reduction of $d_{||}$ band splitting (see text). (f) Temperature-dependent resistance of a pristine film and after electrolyte gating: the gated phase presents reduced resistivity at low temperatures. The small hysteresis is due to the fabrication process or incomplete gating (see Supporting Information).

O 2p states resulting in the π^* band being pushed to higher energy and thereby opening an energy gap in the monoclinic phase, as shown in Figure 1b.[4,10] The strong temperature-driven modulation of the density of states (DOS) at E_F leads to large changes in the transport properties (Figure 1c).

It has long been of interest to induce a metallic state in VO_2 below the MIT temperature, T_{MIT}, for example, by light or by electric fields. Using conventional field-effect transistor geometries in which the channel is formed from VO_2 and gated with conventional gate dielectrics, the electric fields are not sufficiently large to change the electronic state of VO_2. However, using ionic liquid electrolyte gate dielectrics, which provide much larger electric fields at the liquid/channel interface, Jeong *et al.*[8] and Nakano *et al.*[11] have found that a VO_2 channel can be gated to a metallic state below T_{MIT}. However, whereas Nakano *et al.*[11] claimed that the metallic state resulted from a collapse of the Mott insulating energy gap due to electrostatically induced electrons at the oxide surface, Jeong *et al.*[8] showed that the metallic state in the VO_2 channel was non-volatile and persisted when the gate voltage was reduced to zero and even after the ionic liquid was completely removed from the VO_2 surface. Using a wide variety of characterization techniques and studies, Jeong *et al.*[8] provided strong evidence that the metallicity in VO_2 arises from the formation of oxygen vacancies due to an electric-field-induced oxygen migration during the gating process. Moreover, these authors showed this process to be reversible.[8] In the scenario of Jeong *et al.*,[8] there is no reason to expect that the structure of the metallic state of gated VO_2 is the same as that of the thermally induced metallic phase, but Nakano *et al.*[11] claimed that the gate-induced metallic phase has the same rutile structure as that of the high-temperature metallic state. It is thus very important to determine the crystal and electronic structure of the gate-induced metallic phase in VO_2. Here we perform high-energy X-ray photoelectron spectroscopy (HAXPES) on electrolyte-gated VO_2 thin films at various temperatures to elucidate its electronic structure. HAXPES has a key advantage over conventional photoelectron spectroscopy in that high-energy photons excite high kinetic energy electrons which have a long inelastic mean free path and correspondingly large escape depth and thus a high bulk sensitivity.[12−15]

RESULTS

A schematic of the measurement setup and device used is shown in Figure 2a (see Experimental Methods for details). Panels b−e and f,g of Figure 2 show, respectively, the valence band (VB) and the V 2p spectra measured at various photoemission angles and temperatures. Measurements were performed on the same sample in the pristine monoclinic (120 K) and rutile (350 K) phases as well as the gated (120 K) state. The VB spectra from these different states are compared in Figure 2b. The rutile phase is obviously metallic, exhibiting a coherent peak at ~0.3 eV below the Fermi level, consistent with previous work.[9] The

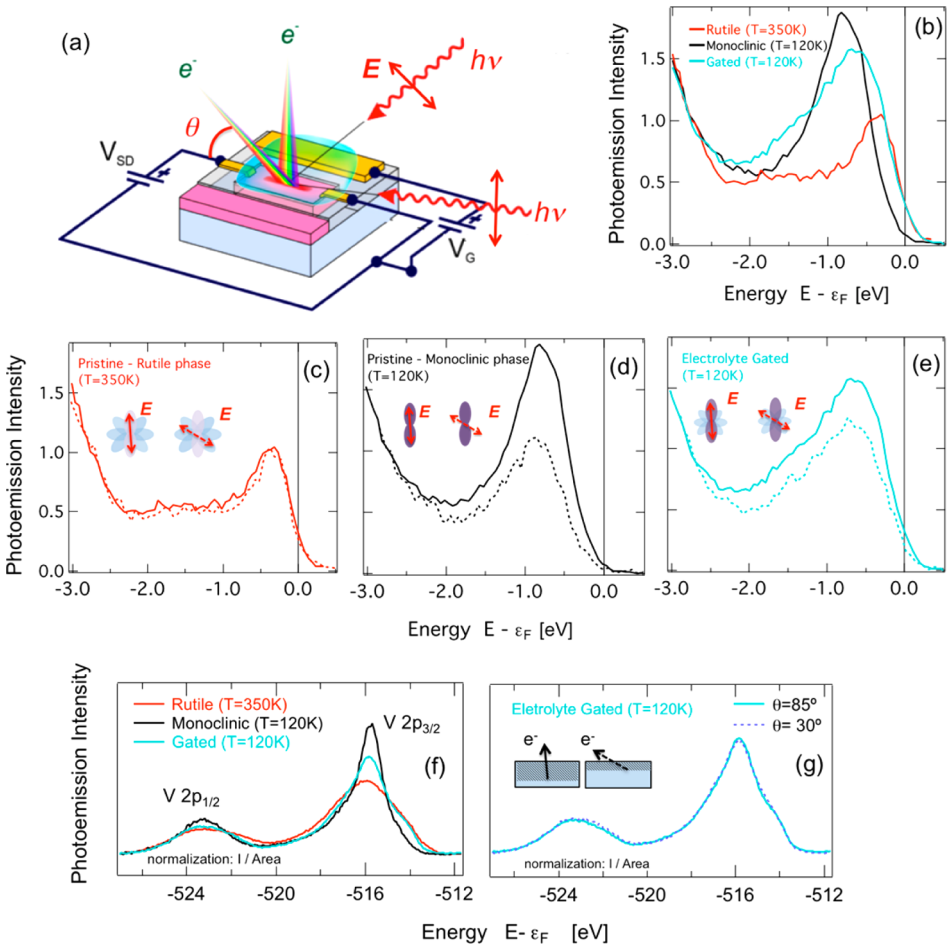

Figure 2. (a) Experiment and device schematic. The gate electrode, with an area of 4 × 10 mm^2, and the electrical contacts to the channel are formed from 5 nm Ru/65 nm Au (yellow). The VO_2 channel (pink) of size 2 × 6 mm^2 is set at a distance 0.5 mm from the gate. The semitransparent turquoise droplet is the ionic liquid. The substrate is shown in blue. The angle between the photon beam and analyzer is fixed at 90°. The linearly π-polarized light impinges the sample at an incidence angle of 5 and 60° for near-normal ($\theta = 85°$) and off-normal ($\theta = 30°$) photoemission measurements, respectively. The largest beam spot size, which is at 5° light incidence, is ~0.1 × 3 mm^2. (b) VB spectra at near-normal emission condition measured at 3.0 keV for VO_2 in the rutile (350 K), gated (120 K), and monoclinic (120 K) states. Subfigures (c−e) show the dependence of the VB spectra intensity on the light incidence for the three phases. Solid (dashed) lines represent the incidence angle of 5° (60°). Insets depict the relationship between orbital polarization and the electric field direction (*E*) of the light in each case. (f) V 2p spectra measured at the same conditions as for (b). Subfigure (g) shows that there is no dependence of the V 2p spectral shape on the photoemission (and light incidence) angle, indicating that the electronic structure of the electrolyte-gated sample extends through a relatively thick region, as illustrated by the inset.

monoclinic structure, on the other hand, shows a peak at ~0.9 eV below E_F.[9] The VB spectrum of the gated structure is broadened in comparison to the monoclinic structure and exhibits a shift to lower binding energy of about 200 meV and additional spectral weight at E_F.

The dependence of the relative photoemission intensity of the 3d bands on the light incidence angle was also investigated. Inspection of the 3d band photoemission (Figure 2b) shows that the intensity at the peak maximum in the monoclinic phase is much higher than that in the rutile phase at the peak maximum for low incidence angles. The 3d band of the gated phase exhibits a peak photoemission intensity between that of the rutile and monoclinic. This behavior may be a consequence of the orbital polarization in this compound.[16] In the rutile phase, the nondimerized V atoms possess a homogeneous spatial distribution of 3d states, as sketched in the inset of Figure 2c. The $d_{\|}$ and π^* states (2p−3d hybridized) are occupied. Therefore, the photoemission intensity does not present a strong dependence on the light electric field direction. By contrast, the monoclinic phase has a strong dimerization of V atoms resulting in a strong orbital polarization. That is, only the $d_{\|}$ band is occupied at energies near E_F. The light electric field at low incident angles couples with the $d_{\|}$ states, resulting in an enhanced photoemission intensity in comparison to high incident angles (Figure 2d). In the gated phase, the angular dependence is smaller, which can be ascribed to a partial orbital polarization (Figure 2e). A smaller orbital polarization is a direct consequence of the reduced V dimerization, as shown schematically in Figure 1d. Indeed, this result is consistent with recent structural measurements of electrolyte-gated VO_2 using *in situ* synchrotron X-ray diffraction.[17]

In Figure 2f, the rutile V $2p_{3/2}$ peak is located at ~515.9 eV, consistent with the V^{4+} oxidation state in VO_2 and is significantly broadened in comparison to the other two peaks.[18] This broadening has been attributed primarily to the absence of V dimerization;[19] metallic screening effects also play a role.[6,9] At low temperatures, the transition to the monoclinic phase can be easily identified by the decreased V $2p_{3/2}$ peak width. The gated film at 120 K presents a similar V $2p_{3/2}$ spectra as the monoclinic phase, with the exception of a shoulder at lower binding energy. Figure 2g shows the gated V 2p spectra measured at different emission angles. Data collected at quasi-normal emission ($\theta = 85°$) have essentially the same features as the off-normal emission ($\theta = 30°$), pointing to the homogeneity of the gated phase over a relatively thick region (>40 Å). Comparison between gated and pristine spectra collected in both photoemission angles for different temperatures can be found in Figure S1.

It is important to note that the spectra for the gated films measured at 120 K cannot be fit as a combination of the monoclinic and rutile spectra (Figure S2). Therefore, the shoulder in the V $2p_{3/2}$ peak and the modifications in the VB after the gating process are due to a structural change, which is different from that observed in the pristine VO_2 monoclinic → rutile structural phase transition. In the gated sample, the shoulder at lower binding energy in the V $2p_{3/2}$ peak is consistent with the presence of vanadium atoms in the +3 valence state; this leads to V $2p_{3/2}$ peaks with larger energy broadening than the pristine monoclinic phase, such as typically found in Magnéli phases.[8,18,19] Additionally, the broadening and shift in the VB spectra of the gated sample is also consistent with the reduced oxygen content in the Magnéli phases, for example, V_5O_9 and V_6O_{11} (Figure S2).[18,19] V_5O_9 and V_6O_{11} have nondimerized and partially dimerized V−V bonds, respectively, and the broadening of the V $2p_{3/2}$ peak and shift in the VB spectra have been attributed to this reduction in V−V dimerization.[19] Based on these observations and the dependence of the VB intensity on light incidence angle, we suggest that the gated structure may also exhibit larger V−V interatomic distances than the monoclinic phase (Figure 1d−f).

Figure 3 compares the spectra from the gated sample measured at temperatures above (350 K) and below (120 K, same as Figure 2b) the MIT of the pristine film. At 350 K, the V 2p spectrum of the gated film resembles that of the pristine rutile structure. This may indicate structural similarities between the rutile phase and the gated phase at high temperature. However, the VB spectra of the gated film at all temperatures show distinct features that are not associated with the rutile or the monoclinic phase, further demonstrating the distinct electronic structure in the gated state.

According to the photoemission spectra measured at different emission angles (Figure 2g), the electronic structure of the gate-induced metallic phase is not

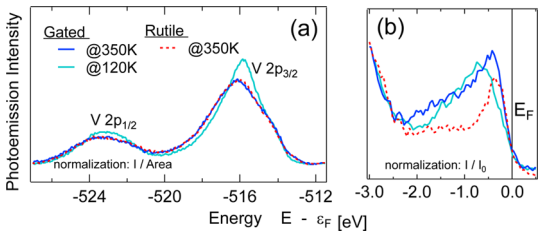

Figure 3. Spectra measured for VO_2 on TiO_2 at 3.0 keV of V 2p (a) and valence bands (b) for rutile (350 K) and gated (120 and 350 K) states. Note that the MIT for the pristine film is 290 K. In (b), $I_0 = I$ (2.8 eV).

limited to the surface, but rather extends to a thickness beyond that examined by HAXPES (here >40 Å). As discussed above, the electronic structure of this phase is consistent with the model of Jeong *et al.*,[8] who have proposed that oxygen vacancies are induced by electrolyte gating of VO_2. To better understand the effect of the formation of oxygen vacancies in the pristine VO_2, density functional theory (DFT) calculations were performed with the VASP[20] program package using the Heyd, Scuseria, and Ernzerhof (HSE) hybrid functional[21] taking 12.5% of exact exchange (labeled as HSE-0.125), the Perdew, Burke, Ernzerhof (PBE) functional,[22] and a rotationally invariant implementation of the PBE+U functional.[23] In the case of PBE+U, the Hubbard on-site repulsion U and J exchange interaction was included using $U_{eff} = U - J = 3.32$ eV in accordance with ref 24 (more details are presented in the Supporting Information). Theoretical efforts to simulate the experimental observations are complicated by the strong electron correlation effects in VO_2.[5,25] This issue notwithstanding, we have applied DFT calculations in a simplified model of the gated phase, in which we concentrate our efforts on capturing general trends in the structural modifications and electronic structure induced by oxygen removal. When O is removed, the structural changes extend far beyond the first coordination shell and are quite substantial in the whole supercell volume (see Figure 4a). Our calculations indicate that, besides the atomic structure, the electronic structure is also strongly affected by oxygen vacancy creation. For an O1-type vacancy (oxygen vacancy between dimerized V atoms), the flow of the bond charge density shows that the two valence electrons of the removed oxygen atom (see the blue isosurface in Figure 4b) are redistributed over the whole volume of the simulation cell (see the red isosurface in Figure 4b). This charge density is rather delocalized and could serve as a charge carrier, leading to conductivity in the oxygen-deficient structure. The calculated DOS computed with either PBE+U or HSE-0.125 hybrid functionals provides qualitatively similar results, showing that compared to pristine VO_2 (Figure 4c), the oxygen vacancies lead to a broadening of the V 3d states and a reduction in the band gap compared to the monoclinic phase (Figure 4d). This

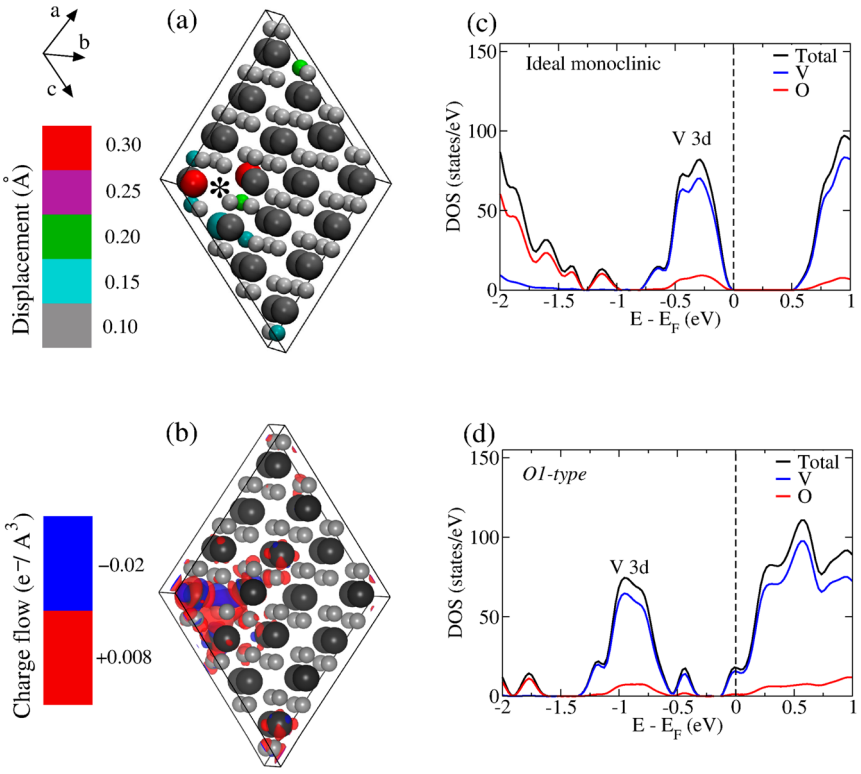

Figure 4. (a) Atomic relaxations around an O1-type vacancy (oxygen vacancy between dimerized V atoms) computed with PBE+U. Relative to the ideal defect-free structure, the displacement of the atoms due to the structural relaxation is represented with different colors in the range of 0.3−0.1 Å. The position of the oxygen defect site is marked with a black star. (b) Redistribution of the electronic charge upon the creation of an O1-type vacancy. Blue and red isosurfaces correspond to charge depletion and accumulation, respectively. The isovalues have been selected such that the isosurfaces enclose about ±70% of the redistributed charge. For clarity, the effect of atomic relaxation was not taken into account. In (a) and (b), the large and small spheres correspond to V and O atoms, respectively. Subfigures (c) and (d) show the total and atom-projected DOS near the Fermi energy for the pristine monoclinic VO_2 and for the case of the O1-type vacancy, respectively. The Fermi energy (E_F) is defined here as the energy level of the highest occupied state at 0 K.

modification in the DOS leads to the emergence of new states in energy positions above the Fermi energy of the monoclinic structure, in agreement with very recent dynamical mean-field theory simulations[26] and with the increased spectral weight near E_F observed in the HAXPES valence band spectra of the gated films (Figure 2c).

CONCLUSION

In summary, valence band and V 2p photoemission spectra reveal that the gate-induced metallic state in VO_2 has a distinct electronic structure from that of the rutile metallic phase of the pristine film. In our experiments, we observe broadening of the valence band in the gated state to lower energies, which we speculate is due to the formation of oxygen vacancies since broadening of the valence band is characteristic of Magnéli phases[18,19] that have reduced oxygen content in comparison to VO_2. We conclude that the monoclinic structure and the associated orbital degeneracy of the insulating phase is retained but modified by electrolyte gating, as summarized schematically in Figure 1d,e. The V−V distance is increased in the gated phase and is consistent with the creation of oxygen vacancies, as proposed by Jeong *et al.* (Figure 1d).[8] Larger V−V distances imply a smaller d orbital overlap, decreasing the $d_{\|}$ band splitting without lifting the orbital polarization. This is accompanied by a charge redistribution due to the removal of oxygen, populating empty states at E_F (Figure 1e). Additionally, the gated sample shows a substantial increase in spectral weight at E_F, reflecting the enhanced conductivity at low temperatures (Figure 1f). The observed electronic structures are consistent with an electrochemical reaction in VO_2 leading to the formation of oxygen vacancies over a relatively thick region, in agreement with the results reported in ref 8.

EXPERIMENTAL METHODS

An epitaxial VO_2 thin film and device were prepared on (001) TiO_2. The VO_2 thin film is 10 nm thick with a MIT temperature of 290 K and a rms roughness of 10 Å. Further details are available in ref 8. An X-ray excitation energy of 3 keV (P09, PETRA III, DESY) was used to study the VO_2 film in its pristine and gated states (120−350 K). At this excitation energy, the probing depth can be varied from ∼40 to ∼20 Å by increasing the angle of emission (θ) from 90° (normal) to 30° (off-normal).[27,28] A linear background was subtracted from the V 2p spectra, which was

then normalized by the V $2p_{3/2}$ area. VB spectra were normalized by the photoemission intensity at the high-energy tail of the O 2p band (energy ~2.8 eV).

The sample was gated by applying $V_G = 2.1$ V at 330 K (above the MIT) and then sweeping the temperature from 330 to 10−330 at 3 K/min. Gating was performed under vacuum *ex situ*, leading to a conducting state (gated VO_2) as evidenced by a conductivity increase of 3 orders of magnitude (Figure 1f). Since Jeong *et al.*[8] have shown that the conducting state in VO_2 persists even after electrolyte removal, HAXPES is used to probe the electronic structure of the gate-induced metallic phase after the liquid electrolyte was removed by washing the sample with isopropyl alcohol. This allowed for measurements of the VB and core states of VO_2 thin films with a high signal-to-noise ratio.

Conflict of Interest: The authors declare no competing financial interest.

Acknowledgment. We gratefully acknowledge A. Hloskovsky (P09, PETRA III) for experimental support. The experiments at PETRA III under proposals I-20120669, I-20120684, and I-20110762 were financially supported by the German Federal Ministry of Education and Research (BMBF, 05K10UMA). The synchrotron radiation measurements at BL47XU were performed with the approval of the Japan Synchrotron Radiation Research Institute (JASRI; Proposal No. 2012B0043).

Supporting Information Available: Temperature-dependent HAXPES, comparison of gated and weighted average spectra, O 2p HAXPES spectra, Magnéli phase valence band comparison, sample transport properties, and *ab initio* calculations. This material is available free of charge *via* the Internet at http://pubs.acs.org.

REFERENCES AND NOTES

1. Dagotto, E. Complexity in Strongly Correlated Electronic Systems. *Science* **2005**, *309*, 257–262.
2. Morin, F. J. Oxides Which Show a Metal-to-Insulator Transition at the Néel Temperature. *Phys. Rev. Lett.* **1959**, *3*, 34.
3. Ilinskiy, A. V.; Kvashenkina, O. E.; Shadrin, E. B. Nature of the Electronic Component of the Thermal Phase Transition in VO_2 Films. *Semiconductors* **2012**, *46*, 1171–1185.
4. Eyert, V. The Metal−Insulator Transitions of VO_2: A Band Theoretical Approach. *Ann. Phys.* **2002**, *11*, 650–702.
5. Eyert, V. VO_2: A Novel View from Band Theory. *Phys. Rev. Lett.* **2011**, *107*, 016401.
6. Eguchi, R.; Taguchi, M.; Matsunami, M.; Horiba, K.; Yamamoto, K.; Ishida, Y.; Chainani, A.; Takata, Y.; Yabashi, M.; Miwa, D.; *et al.* Photoemission Evidence for a Mott−Hubbard Metal−Insulator Transition in VO_2. *Phys. Rev. B* **2008**, *78*, 075115-6.
7. Kanki, T.; Takami, H.; Ueda, S.; Hattori, A. N.; Hattori, K.; Daimon, H.; Kobayashi, K.; Tanaka, H. Identifying Valence Band Structure of Transient Phase in VO_2 Thin Film by Hard X-ray Photoemission. *Phys. Rev. B* **2011**, *84*, 085107.
8. Jeong, J.; Aetukuri, N.; Graf, T.; Schladt, T. D.; Samant, M. G.; Parkin, S. S. P. Suppression of Metal−Insulator Transition in VO_2 by Electric Field-Induced Oxygen Vacancy Formation. *Science* **2013**, *339*, 1402–1405.
9. Suga, S.; Sekiyama, A.; Imada, S.; Miyamachi, T.; Fujiwara, H.; Yamasaki, A.; Yoshimura, K.; Okada, K.; Yabashi, M.; Tamasaku, K.; *et al.* ~8 keV Photoemission of the Metal−Insulator Transition System VO_2. *New J. Phys.* **2009**, *11*, 103015.
10. Aetukuri, N. B.; Gray, A. X.; Drouard, M.; Cossale, M.; Gao, L.; Reid, A. H.; Kukreja, R.; Ohldag, H.; Jenkins, C. A.; Arenholz, E.; *et al.* Control of the Metal−Insulator Transition in Vanadium Dioxide by Modifying Orbital Occupancy. *Nat. Phys.* **2013**, *9*, 661–666.
11. Nakano, M.; Shibuya, K.; Okuyama, D.; Hatano, T.; Ono, S.; Kawasaki, M.; Iwasa, Y.; Tokura, Y. Collective Bulk Carrier Delocalization Driven by Electrostatic Surface Charge Accumulation. *Nature* **2012**, *487*, 459–462.
12. Feng, D.-L. Photoemission Spectroscopy: Deep into the Bulk. *Nat. Mater.* **2011**, *10*, 729–730.
13. Gray, A. X.; Papp, C.; Ueda, S.; Balke, B.; Yamashita, Y.; Plucinski, L.; Minár, J.; Braun, J.; Ylvisaker, E. R.; Schneider, C. M.; *et al.* Probing Bulk Electronic Structure with Hard X-ray Angle-Resolved Photoemission. *Nat. Mater.* **2011**, *10*, 759–764.
14. Lindau, I.; Pianetta, P.; Doniach, S.; Spicer, W. E. X-ray Photoemission Spectroscopy. *Nature* **1974**, *250*, 214–215.
15. Sekiyama, A.; Iwasaki, T.; Matsuda, K.; Saitoh, Y.; Ônuki, Y.; Suga, S. Probing Bulk States of Correlated Electron Systems by High-Resolution Resonance Photoemission. *Nature* **2000**, *403*, 396–398.
16. Haverkort, M. W.; Hu, Z.; Tanaka, A.; Reichelt, W.; Streltsov, S. V.; Korotin, M. A.; Anisimov, V. I.; Hsieh, H. H.; Lin, H. J.; Chen, C. T.; *et al.* Orbital-Assisted Metal−Insulator Transition in VO_2. *Phys. Rev. Lett.* **2005**, *95*, 196404.
17. Jeong, J.; Aetukuri, N. B.; Passarello, D.; Conradson, S. D.; Samant, M. G.; Parkin, S. S. P. Giant Reversible Structural Changes in a Correlated-Electron Insulator Induced by Ionic Liquid Gating. Submitted for publication.
18. Mendialdua, J.; Casanova, R.; Barbaux, Y. XPS Studies of V_2O_5, V_6O_{13}, VO_2 and V_2O_3. *J. Electron Spectrosc. Relat. Phenom.* **1995**, *71*, 249–261.
19. Obara, M.; Sekiyama, A.; Imada, S.; Yamaguchi, J.; Miyamachi, T.; Balashov, T.; Wulfhekel, W.; Yabashi, M.; Tamasaku, K.; Higashiya, A.; *et al.* V−V Dimerization Effects on Bulk-Sensitive Hard X-ray Photoemission Spectra for Magnéli Phase Vanadium Oxides. *Phys. Rev. B* **2010**, *81*, 113107.
20. Kresse, G.; Furthmüller, J. Efficient Iterative Schemes for *Ab Initio* Total-Energy Calculations Using a Plane-Wave Basis Set. *Phys. Rev. B* **1996**, *54*, 11169–11186.
21. Heyd, J.; Scuseria, G. E.; Ernzerhof, M. Hybrid Functionals Based on a Screened Coulomb Potential. *J. Chem. Phys.* **2003**, *118*, 8207–8215.
22. Perdew, J. P.; Burke, K.; Ernzerhof, M. Generalized Gradient Approximation Made Simple. *Phys. Rev. Lett.* **1996**, *77*, 3865–3868.
23. Dudarev, S. L.; Botton, G. A.; Savrasov, S. Y.; Humphreys, C. J.; Sutton, A. P. Electron-Energy-Loss Spectra and the Structural Stability of Nickel Oxide: An Lsda+U Study. *Phys. Rev. B* **1998**, *57*, 1505–1509.
24. Appavoo, K.; Lei, D. Y.; Sonnefraud, Y.; Wang, B.; Pantelides, S. T.; Maier, S. A.; Haglund, R. F. Role of Defects in the Phase Transition of VO_2 Nanoparticles Probed by Plasmon Resonance Spectroscopy. *Nano Lett.* **2012**, *12*, 780–786.
25. Grau-Crespo, R.; Wang, H.; Schwingenschlögl, U. Why the Heyd−Scuseria−Ernzerhof Hybrid Functional Description of VO_2 Phases Is Not Correct. *Phys. Rev. B* **2012**, *86*, 081101.
26. Weber, C.; O'Regan, D. D.; Hine, N. D. M.; Payne, M. C.; Kotliar, G.; Littlewood, P. B. Vanadium Dioxide: A Peierls−Mott Insulator Stable against Disorder. *Phys. Rev. Lett.* **2012**, *108*, 256402.
27. Powell, C. J.; Jablonski, A.; Tilinin, I. S.; Tanuma, S.; Penn, D. R. Surface Sensitivity of Auger-Electron Spectroscopy and X-ray Photoelectron Spectroscopy. *J. Electron Spectrosc. Relat. Phenom.* **1999**, *98−99*, 1–15.
28. Tanuma, S.; Powell, C. J.; Penn, D. R. Calculations of Electron Inelastic Mean Free Paths VIII. Data for 15 Elemental Solids over the 50−2000 eV Range. *Surf. Interface Anal.* **2005**, *37*, 1–14.